# Ground-Motion Prediction Equations for Constant-Ductility Input Energy Spectra

# Yin Cheng[1], Andrea Lucchini[2], Fabrizio Mollaioli[3]

**[1] School of Civil Engineering, Southwest Jiaotong University,**
**No. 111, North 1st Section, 2nd Ring Road, Chengdu, Sichuan, China**

**[2,3] Department of Structural and Geotechnical Engineering, Sapienza University of Rome,**
**Via Gramsci 53, I-00197 Rome, Italy**

## Abstract

With energy-based seismic design methods, the effect of earthquakes on structures in terms of both force and displacement demand can be taken into account, as well as the cumulative effect of cyclic loading. The elastic input energy, which accounts for frequency content, duration and amplitude of the ground motion, was shown to be a good predictor of the structural response. The inelastic input energy, however, can better predict the response of structures that experience damage when subjected to the seismic excitation. Establishing ground motion prediction equations for inelastic input energy spectra is therefore a target of great interest in earthquake engineering. New ground motion prediction equations are proposed in this study for constant-ductility input energy spectra. The proposed equations are developed using mixed-effects models calibrated through empirical regressions on a large number of strong motions. Parametric analyses are carried out to show the effect of some properties variation, such as fault mechanism and type of soil, on the considered parameters.

*Keywords: Seismic Intensity Measures, Constant-Ductility Input Energy Spectra, Ground Motion Prediction Equation, Performance-Based Earthquake Engineering.*

## 1. Introduction

Several seismic intensity measures (IMs) have been proposed to estimate and characterize the damage potential of strong ground motions. Currently, the most widely used IMs in Performance Based Earthquake Engineering (PBEE) are the pseudo-acceleration ($S_a$), the pseudo-velocity ($S_v$), and peak ground acceleration (PGA) or velocity (PGV). More recently, also parameters defined in terms of the displacement response of single-degree-of-freedom (SDOF) systems have been proposed. With respect to strength and displacement based design methods, energy based methods make use of IMs that characterize also the duration and the frequency content of the seismic excitation, representing therefore those

properties of the ground motion that are strongly related to the destructive potential of earthquakes. These latter design methods require definition of the design seismic action in terms of energy, and evaluation of the absorption and dissipation capacity of the structure. Housner [1], Akyiama [2], and Uang and Bertero [3] are the first researchers that introduced energy concepts in structural seismic design. After them, starting from the late 1990's, extensive studies were carried out on energy [4-12]. In particular, Decanini and Mollaioli [5] introduced a methodology to determine elastic design input energy spectra as functions of earthquake magnitude, site-to-source distance, and site soil conditions. Further studies [6, 7] developed attenuation relationships for input energy parameters. Furthermore, Manfredi [8] and Decanini and Mollaioli [9] discussed the importance of hysteretic energy in characterizing the energy demand due to earthquakes. Finally, Mollaioli et al. [12] analyzed the correlation between displacement and energy spectra for single- and multiple-degree-of-freedom systems.

Recently, it was shown [13, 14] the significant predictive capability of energy based IMs, providing an improved basis to define seismic hazard. New ground motion prediction equations (GMPEs) have been established for the absolute and the relative elastic input energy equivalent velocities [15], on the basis of a large set of strong ground motions. Moreover, correlation coefficients between the response spectral values of input energy equivalent velocities corresponding to different periods and components of the ground motion have been evaluated [16], in order to gain information about of their joint occurrence.

However, since structures generally go into nonlinear range of response when subjected to strong ground motions, inelastic input energy spectra are required to better predict the structural response. Aim of this study is to establish new GMPEs for the absolute and the relative constant-ductility input energy spectra. The latter are

expressed in terms of the geometric mean of the input energy equivalent velocities of the two horizontal components of the ground motion. A mixed-effects model for considering the energy variation of records within a single event and between different events is employed in regression analyses for the development of the prediction equations.

## 2. Input energy equivalent velocities

For an elastic damped SDOF system subjected to the earthquake ground motion the energy balance equation [3] can be used to express the (absolute or relative) input energy ( $E_{Ia}$, or $E_{Ir}$, respectively) as follows

$$E_{Ia,r}(t)=E_k(t)+E_s(t)+E_H(t)+E_\xi(t) \qquad (1)$$

where $E_k(t)$, $E_s(t)$, $E_H(t)$ and $E_\xi(t)$, denote the kinetic energy (absolute or relative), the elastic strain energy, the hysteretic energy and the damping energy, respectively.

The two different input energies are defined as: the absolute input energy $E_{Ia}$ (equal to the work done by the total force applied to the base of the SDOF system in the ground displacement), and the relative input energy $E_{Ir}$ (equal to the work done by the static equivalent force in the displacement of the equivalent fixed-base SDOF system relative to the ground).

In order to eliminate the dependence on mass, these two energy parameters can be conveniently converted into equivalent velocities using the following equation:

$$V=\sqrt{2E/m} \qquad (2)$$

The absolute and the relative input energy equivalent velocities can be consequently defined as follows:

$$V_{EIa}=\sqrt{2E_{Ia}/m} \qquad (3)$$

$$V_{EIr}=\sqrt{2E_{Ir}/m} \qquad (4)$$

With the increase of the period of the SDOF system, $V_{EIa}$ approaches zero whereas $V_{EIr}$ points toward the maximum ground velocity. At decreasing periods, instead, $V_{EIr}$ approaches zero while $V_{EIa}$ approaches the maximum ground velocity. Regardless of the considered period of the SDOF system, $V_{EIa}$ and $V_{EIr}$ converge to almost the same value at the end of the ground motion duration.

## 3. Regression analysis on strong motion data

1227 ground motions from 60 main shock earthquakes are selected from the NGA database and used to derive the proposed GMPEs in this study. Each of them represents a

free-field motion, has two horizontal components and is characterized by a measured or estimated $V_{S30}$. Criteria similar to those used by Campbell and Bozorgnia [17] are adopted to select the records employed for deriving the prediction equations. Only earthquakes located within the shallow continental crust in a tectonically active region are selected. The distribution of the selected ground motions with respect to moment magnitude and site-rupture closest distance (rupture distance) is shown in Fig. 1. A summary of these earthquakes is also given in [15].
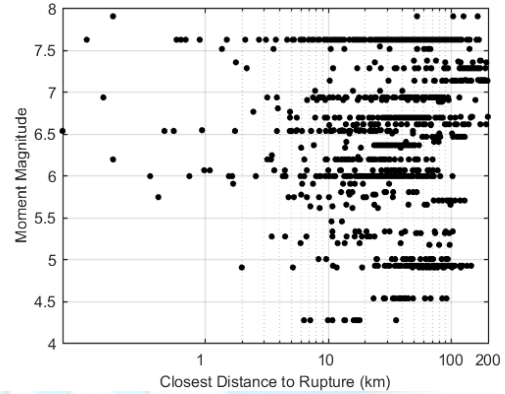


Fig. 1 Magnitude-distance distribution of the ground motions used in the study.

The mixed-effects model [18] is applied in regression analyses to estimate the unknown coefficients of the GMPEs, so as to account for both fixed and random effects. By using this method, correlations within sample subgroups of data are recognized and represented with additional error terms in the predictive equation as follows:

$$\ln(IM_{ij})=f(M_i,R_{ij},V_{S30ij},NR_i,RS_i,\theta)+\eta_i+\varepsilon_{ij} \qquad (5)$$

where $IM_{ij}$ is the considered IM (i.e., $V_{EIa}$ or $V_{EIr}$) value for the j-th record and the i-th event, $M_i$ is the moment magnitude of the i-th event, $R_{ij}$ is the closest distance to rupture from the i-th event to the station of the j-th recording, and $V_{S30}$ is the value of the average shear-wave velocity in the upper 30 meters. The variables NR and RS are defined as follows: NR=1 for normal fault mechanism and normal-oblique, 0 otherwise; RS=1 for reverse fault and reverse-oblique mechanism, 0 otherwise; NR=0 and RS=0 for strike-slip fault mechanism.

The NLME (Nonlinear Mixed-Effects model) package implemented in the statistical software R [19] is employed for calibrating the model.

## 4. Proposed prediction equations

The specific functional form, originally proposed by Boore

et al. [20] and used for the prediction of both $V_{EIa}$ and $V_{EIr}$ in this study, is:

$$\ln(IM_{ij})=a+b(M_i-6)+c(M_i-6)^2+(d+fM_i)\ln\sqrt{R_{ij}^2+h^2}+e\ln(V_{S30ij}/1130) \quad (6)$$
$$+m1NR_i+m2RS_i+\eta_i+\varepsilon_{ij}$$

Fig. 2 reports the normal Quantile-Quantile plots for the residuals of $V_{EIa}$ obtained in the case of a constant-ductility value equal to 4. These plots show that both total and intra-event residuals have a very good fit to the assumed normal distribution. Similar trends, not shown here for the sake of brevity, characterize also the regression residuals of $V_{EIa}$ and $V_{EIr}$ obtained for other ductility values. Fig. 3 shows the light dependence of inter-event residuals of $V_{EIa}$ on moment magnitude. Figures from 4 to 6 show the dependence of intra-event residuals of $V_{EIa}$ (again, for a constant ductility of 4) on magnitude, distance and $V_{S30}$. No significant trend or bias is observed, confirming that the used function can be considered appropriate for the selected predictor variables.
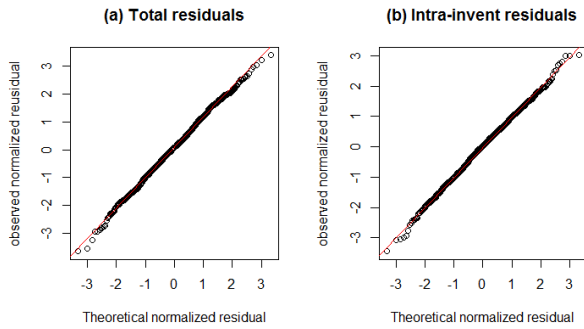


Fig. 2  Normal Q-Q plot for the residuals of $V_{EIa}$ for a constant-ductility of 4, obtained using the proposed GMPE.
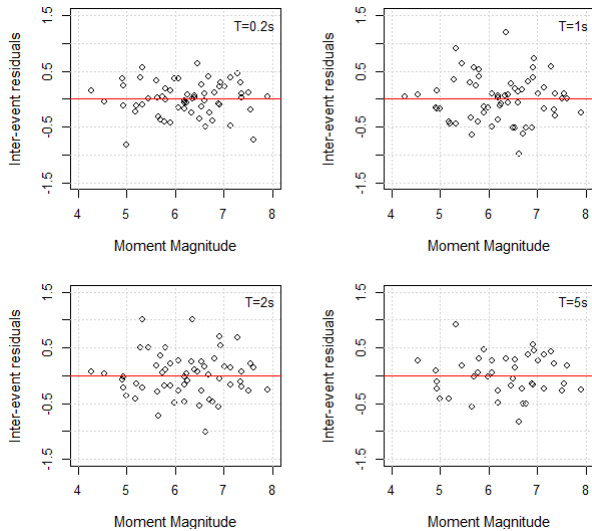


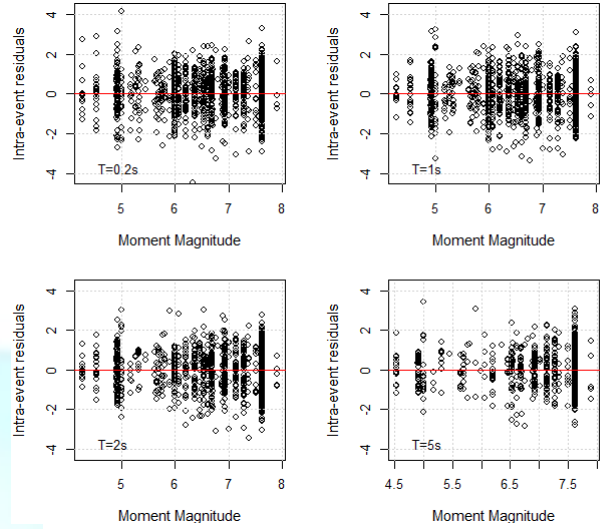Fig. 3 Dependence of inter-event residuals of $V_{EIa}$ on magnitude.



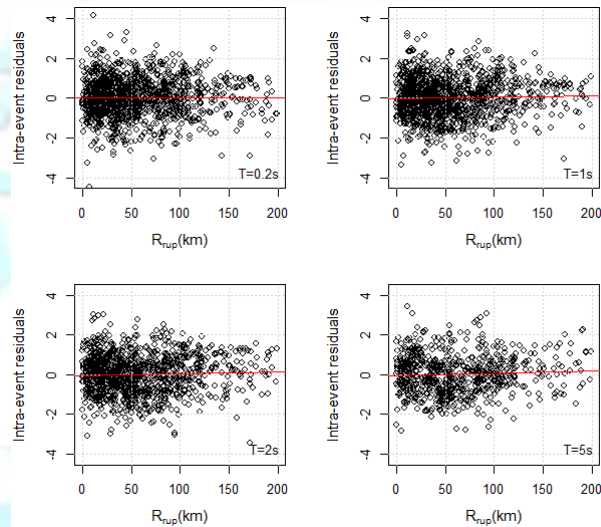Fig. 4  Dependence of intra-event residuals of $V_{EIa}$ on magnitude.



Fig. 5  Dependence of intra-event residuals of $V_{EIa}$ on rupture distance.
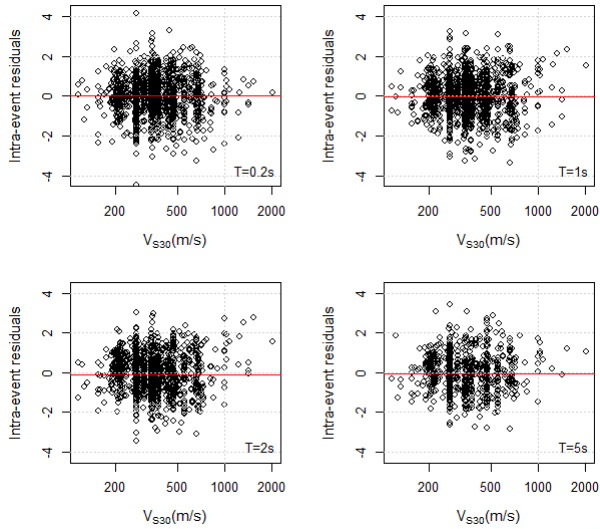
Fig. 6 Dependence of intra-event residuals of $V_{EIa}$ on $V_{S30}$.

In Appendix, the results of the regression analyses on $V_{EIa}$ and $V_{EIr}$ values obtained for a damping ratio of 5% and a ductility (μ) value equal to 2 and 4 are reported. Note that predictive equations for spectra corresponding to different values of the damping can be established by simply recalibrating the regression coefficients.

Fig. 7 reports $V_{EIa}$ and $V_{EIr}$ spectra predicted with the proposed GMPEs for the case of μ=4, M=6.5, R=30 km, and by changing the soil condition and the fault mechanism. By looking at these plots it can be observed that soil condition significantly affects both $V_{EIa}$ and $V_{EIr}$. The two velocities show the same trend with magnitude. For both of them, indeed, the intensity produced by an earthquake with a strike-slip fault mechanism ranges in between the intensities corresponding to normal and reverse-faulting earthquakes.
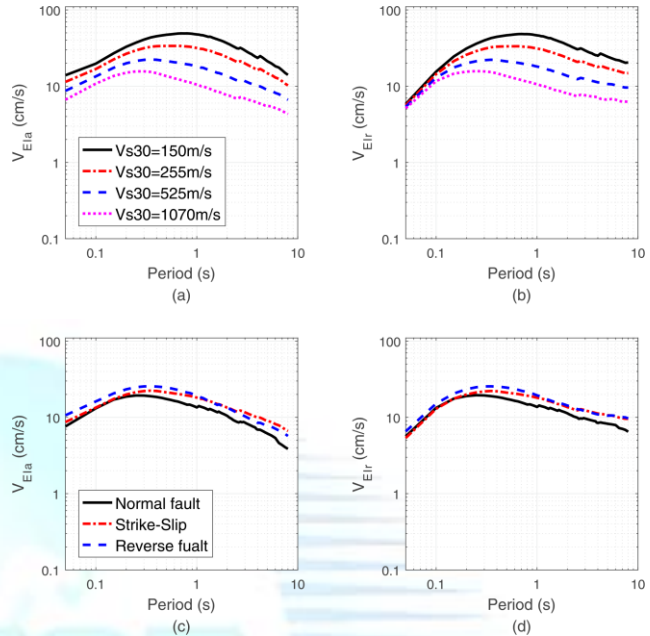


Fig.7 $V_{EIa}$ and $V_{EIr}$ spectra corresponding to μ=4 predicted for the case of M=6.5, R=30 km, and different soil conditions (panels a and b) and fault mechanisms (panels c and d); a strike-slip fault mechanism is considered for spectra in panels a and b, and a $V_{S30}$ value of 525 m/s for those in panels c and d.

$V_{EIa}$ spectra corresponding to different μ values at a site with $V_{S30}$ of 255 m/s and 1070 m/s are shown in Fig. 8 (a) and (c), respectively. Similar spectra but for $V_{EIr}$ are reported in Fig. 8 (b) and (d). It can be noticed that the inelastic spectra have the same spectral shape of the elastic ones. The latter, reported in this figure for comparison, are calculated in accordance with [15]. The two velocities are both sensitive to the ductility level, especially $V_{EIr}$ at short periods. In particular, the velocities' intensity increases with the increase of the ductility value at short periods. An opposite trend is observed in the long period range. Finally, results of parametric analyses not reported here show that the period value at which the elastic and inelastic velocities have the same intensity decreases with the increase of $V_{S30}$.
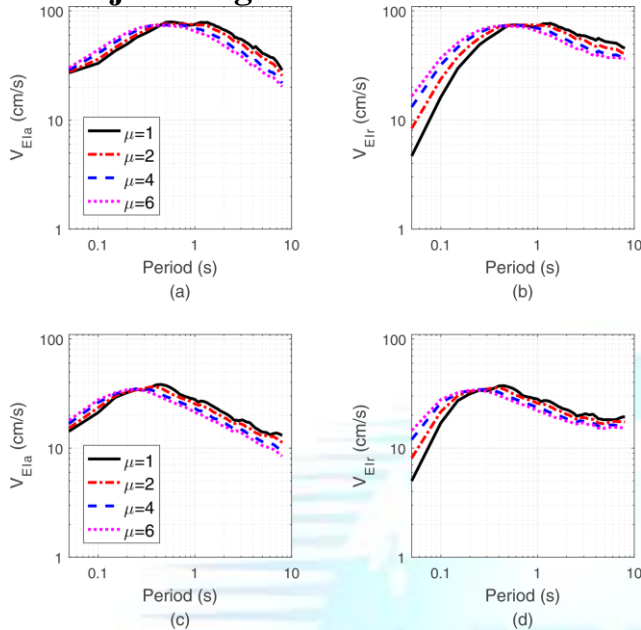
Fig. 8 Comparison between $V_{EIa}$ and $V_{EIr}$ spectra corresponding to different ductilities, produced by a strike-slip earthquake with M=6.5, R=10 km, and a site characterized by a $V_{S30}$ value of 255 m/s (panels a and b) and 1070 m/s (panels c and d).

## 4. Conclusions

For energy based methods the inelastic input energy can be considered a key design parameter for structures exhibiting a nonlinear response to earthquakes. Recent studies have shown that the absolute input energy equivalent velocity $V_{EIa}$ and the relative input energy equivalent velocity $V_{EIr}$ are good alternatives with respect to intensity measures commonly used in performance-based seismic design, as they are able to characterized duration, amplitude and frequency content of the ground motion, as well as and dynamic properties of the structure. In the present paper, ground motion prediction equations developed based on a mixed-effect model have been proposed for estimating the inelastic input energy in terms of the equivalent velocity $V_{EIa}$ and $V_{EIr}$. The proposed equations have been developed using a large number of records characterized by a wide range of magnitude and distance values, and including also a $V_{S30}$ term for the characterization of the soil condition. The equations also include terms to explicitly account for different types of fault mechanisms.

## Appendix

Table 1: Results of the regression analyses on $V_{EIa}$ for $\mu=2$

| T[s] | a | b | c | d | e | f | h | m1 | m2 | τ | σ | $\sigma_T$ |
|------|------|------|--------|--------|--------|-------|-------|--------|--------|-------|-------|-------|
| 0.10 | 5.284 | 0.304 | -0.103 | -1.978 | -0.299 | 0.161 | 5.440 | -0.039 | 0.199 | 0.185 | 0.440 | 0.477 |
| 0.20 | 5.407 | 0.592 | -0.147 | -1.408 | -0.351 | 0.081 | 6.639 | -0.005 | 0.168 | 0.171 | 0.422 | 0.456 |
| 0.30 | 5.286 | 0.683 | -0.165 | -1.253 | -0.434 | 0.064 | 5.945 | -0.092 | 0.164 | 0.188 | 0.445 | 0.483 |
| 0.40 | 5.270 | 0.696 | -0.173 | -1.335 | -0.496 | 0.079 | 5.629 | -0.163 | 0.120 | 0.205 | 0.464 | 0.507 |
| 0.50 | 5.087 | 0.682 | -0.180 | -1.407 | -0.571 | 0.095 | 4.762 | -0.192 | 0.140 | 0.212 | 0.480 | 0.525 |
| 0.60 | 4.906 | 0.685 | -0.188 | -1.445 | -0.627 | 0.105 | 3.869 | -0.201 | 0.155 | 0.221 | 0.493 | 0.540 |
| 0.70 | 4.815 | 0.678 | -0.195 | -1.513 | -0.669 | 0.117 | 3.465 | -0.204 | 0.149 | 0.230 | 0.499 | 0.549 |
| 0.80 | 4.759 | 0.684 | -0.201 | -1.563 | -0.698 | 0.125 | 3.360 | -0.229 | 0.137 | 0.240 | 0.504 | 0.558 |
| 0.90 | 4.714 | 0.689 | -0.214 | -1.608 | -0.722 | 0.132 | 3.266 | -0.230 | 0.127 | 0.250 | 0.507 | 0.566 |
| 1.00 | 4.652 | 0.705 | -0.224 | -1.636 | -0.749 | 0.137 | 3.194 | -0.253 | 0.112 | 0.262 | 0.509 | 0.572 |
| 1.10 | 4.581 | 0.764 | -0.234 | -1.595 | -0.768 | 0.131 | 3.172 | -0.226 | 0.091 | 0.267 | 0.510 | 0.575 |
| 1.20 | 4.574 | 0.793 | -0.243 | -1.600 | -0.773 | 0.132 | 3.353 | -0.252 | 0.060 | 0.267 | 0.511 | 0.576 |
| 1.30 | 4.516 | 0.844 | -0.243 | -1.560 | -0.787 | 0.125 | 3.426 | -0.267 | 0.035 | 0.264 | 0.513 | 0.577 |
| 1.40 | 4.471 | 0.876 | -0.249 | -1.541 | -0.798 | 0.122 | 3.409 | -0.242 | 0.015 | 0.264 | 0.515 | 0.579 |
| 1.50 | 4.402 | 0.915 | -0.246 | -1.515 | -0.805 | 0.118 | 3.349 | -0.239 | 0.004 | 0.263 | 0.512 | 0.575 |
| 1.60 | 4.347 | 0.949 | -0.242 | -1.494 | -0.810 | 0.115 | 3.331 | -0.248 | -0.004 | 0.261 | 0.512 | 0.575 |
| 1.70 | 4.321 | 0.961 | -0.256 | -1.480 | -0.805 | 0.114 | 3.247 | -0.236 | 0.011 | 0.265 | 0.509 | 0.574 |
| 1.80 | 4.291 | 0.975 | -0.247 | -1.494 | -0.812 | 0.115 | 3.303 | -0.237 | 0.008 | 0.263 | 0.509 | 0.573 |
| 1.90 | 4.255 | 1.003 | -0.246 | -1.480 | -0.817 | 0.112 | 3.351 | -0.249 | 0.000 | 0.259 | 0.511 | 0.573 |
| 2.00 | 4.229 | 1.023 | -0.241 | -1.477 | -0.821 | 0.111 | 3.460 | -0.246 | -0.009 | 0.259 | 0.514 | 0.575 |
| 2.20 | 4.191 | 1.056 | -0.230 | -1.476 | -0.818 | 0.110 | 3.565 | -0.276 | -0.009 | 0.260 | 0.519 | 0.580 |
| 2.40 | 4.117 | 1.093 | -0.217 | -1.448 | -0.812 | 0.105 | 3.568 | -0.306 | -0.008 | 0.259 | 0.521 | 0.582 |
| 2.60 | 3.965 | 1.242 | -0.232 | -1.224 | -0.786 | 0.074 | 3.572 | -0.327 | -0.034 | 0.265 | 0.524 | 0.587 |
| 2.80 | 3.965 | 1.303 | -0.250 | -1.191 | -0.782 | 0.069 | 3.940 | -0.332 | -0.085 | 0.273 | 0.526 | 0.592 |
| 3.00 | 3.951 | 1.344 | -0.241 | -1.174 | -0.772 | 0.065 | 4.120 | -0.307 | -0.104 | 0.258 | 0.530 | 0.589 |
| 3.50 | 3.802 | 1.455 | -0.226 | -1.050 | -0.748 | 0.047 | 4.433 | -0.300 | -0.122 | 0.252 | 0.539 | 0.595 |
| 4.00 | 3.692 | 1.502 | -0.208 | -0.982 | -0.724 | 0.038 | 4.516 | -0.345 | -0.148 | 0.250 | 0.550 | 0.604 |
| 4.50 | 3.590 | 1.591 | -0.218 | -0.895 | -0.758 | 0.024 | 4.433 | -0.361 | -0.162 | 0.269 | 0.556 | 0.618 |
| 5.00 | 3.527 | 1.627 | -0.202 | -0.858 | -0.734 | 0.018 | 4.584 | -0.352 | -0.180 | 0.270 | 0.555 | 0.618 |
| 5.50 | 3.560 | 1.640 | -0.207 | -0.875 | -0.703 | 0.020 | 4.836 | -0.389 | -0.190 | 0.280 | 0.552 | 0.619 |

www.ijreat.org

| 6.00 | 3.629 | 1.581 | -0.194 | -0.996 | -0.676 | 0.035 | 5.074 | -0.408 | -0.199 | 0.275 | 0.556 | 0.621 |

Table 2: Results of the regression analyses on $V_{EIa}$ for $\mu=4$

| T[s] | a | b | c | d | e | f | h | m1 | m2 | $\tau$ | $\sigma$ | $\sigma_T$ |
|---|---|---|---|---|---|---|---|---|---|---|---|---|
| 0.10 | 5.345 | 0.384 | -0.115 | -1.775 | -0.307 | 0.132 | 6.017 | -0.022 | 0.186 | 0.170 | 0.425 | 0.458 |
| 0.20 | 5.337 | 0.663 | -0.160 | -1.294 | -0.398 | 0.067 | 6.533 | -0.063 | 0.157 | 0.175 | 0.423 | 0.458 |
| 0.30 | 5.245 | 0.683 | -0.173 | -1.342 | -0.489 | 0.080 | 5.815 | -0.136 | 0.141 | 0.195 | 0.448 | 0.488 |
| 0.40 | 5.073 | 0.682 | -0.181 | -1.416 | -0.567 | 0.096 | 4.881 | -0.181 | 0.133 | 0.209 | 0.465 | 0.510 |
| 0.50 | 4.877 | 0.684 | -0.186 | -1.474 | -0.636 | 0.109 | 4.013 | -0.201 | 0.143 | 0.222 | 0.476 | 0.525 |
| 0.60 | 4.766 | 0.696 | -0.195 | -1.528 | -0.683 | 0.119 | 3.522 | -0.224 | 0.132 | 0.234 | 0.485 | 0.538 |
| 0.70 | 4.700 | 0.710 | -0.201 | -1.571 | -0.718 | 0.126 | 3.433 | -0.248 | 0.108 | 0.243 | 0.491 | 0.548 |
| 0.80 | 4.643 | 0.726 | -0.207 | -1.612 | -0.744 | 0.132 | 3.369 | -0.277 | 0.090 | 0.251 | 0.496 | 0.556 |
| 0.90 | 4.582 | 0.757 | -0.215 | -1.609 | -0.758 | 0.132 | 3.386 | -0.274 | 0.079 | 0.249 | 0.497 | 0.556 |
| 1.00 | 4.520 | 0.804 | -0.215 | -1.588 | -0.770 | 0.129 | 3.351 | -0.297 | 0.057 | 0.251 | 0.498 | 0.558 |
| 1.10 | 4.432 | 0.857 | -0.218 | -1.548 | -0.784 | 0.123 | 3.306 | -0.239 | 0.042 | 0.251 | 0.499 | 0.559 |
| 1.20 | 4.418 | 0.884 | -0.219 | -1.551 | -0.786 | 0.123 | 3.418 | -0.254 | 0.020 | 0.251 | 0.500 | 0.559 |
| 1.30 | 4.357 | 0.923 | -0.213 | -1.526 | -0.796 | 0.118 | 3.421 | -0.262 | 0.007 | 0.249 | 0.500 | 0.559 |
| 1.40 | 4.318 | 0.951 | -0.214 | -1.514 | -0.805 | 0.116 | 3.529 | -0.236 | -0.008 | 0.252 | 0.501 | 0.561 |
| 1.50 | 4.258 | 0.989 | -0.210 | -1.480 | -0.806 | 0.111 | 3.536 | -0.241 | -0.016 | 0.247 | 0.501 | 0.559 |
| 1.60 | 4.217 | 1.018 | -0.203 | -1.461 | -0.809 | 0.108 | 3.597 | -0.246 | -0.029 | 0.245 | 0.503 | 0.560 |
| 1.70 | 4.212 | 1.024 | -0.211 | -1.458 | -0.800 | 0.107 | 3.713 | -0.233 | -0.009 | 0.246 | 0.505 | 0.561 |
| 1.80 | 4.188 | 1.044 | -0.204 | -1.458 | -0.802 | 0.106 | 3.850 | -0.240 | -0.013 | 0.244 | 0.507 | 0.563 |
| 1.90 | 4.159 | 1.063 | -0.199 | -1.448 | -0.800 | 0.104 | 3.939 | -0.241 | -0.014 | 0.242 | 0.509 | 0.564 |
| 2.00 | 4.124 | 1.083 | -0.193 | -1.434 | -0.800 | 0.102 | 4.002 | -0.244 | -0.018 | 0.239 | 0.512 | 0.565 |
| 2.20 | 4.079 | 1.115 | -0.182 | -1.413 | -0.785 | 0.098 | 4.080 | -0.286 | -0.018 | 0.236 | 0.517 | 0.569 |
| 2.40 | 4.016 | 1.147 | -0.170 | -1.384 | -0.780 | 0.094 | 4.176 | -0.307 | -0.027 | 0.234 | 0.518 | 0.569 |
| 2.60 | 3.867 | 1.294 | -0.192 | -1.161 | -0.760 | 0.063 | 4.206 | -0.336 | -0.061 | 0.240 | 0.522 | 0.574 |
| 2.80 | 3.861 | 1.334 | -0.214 | -1.138 | -0.752 | 0.060 | 4.371 | -0.339 | -0.108 | 0.249 | 0.523 | 0.579 |
| 3.00 | 3.820 | 1.360 | -0.205 | -1.123 | -0.738 | 0.057 | 4.323 | -0.310 | -0.121 | 0.242 | 0.527 | 0.580 |
| 3.50 | 3.676 | 1.433 | -0.196 | -1.025 | -0.717 | 0.044 | 4.349 | -0.325 | -0.132 | 0.249 | 0.531 | 0.587 |
| 4.00 | 3.570 | 1.460 | -0.181 | -0.970 | -0.688 | 0.037 | 4.249 | -0.360 | -0.153 | 0.249 | 0.537 | 0.592 |
| 4.50 | 3.455 | 1.552 | -0.192 | -0.878 | -0.720 | 0.023 | 4.318 | -0.370 | -0.155 | 0.254 | 0.538 | 0.595 |
| 5.00 | 3.390 | 1.563 | -0.179 | -0.852 | -0.689 | 0.020 | 4.340 | -0.377 | -0.162 | 0.257 | 0.537 | 0.596 |
| 5.50 | 3.420 | 1.540 | -0.188 | -0.902 | -0.657 | 0.027 | 4.465 | -0.410 | -0.146 | 0.274 | 0.534 | 0.600 |
| 6.00 | 3.476 | 1.442 | -0.176 | -1.067 | -0.644 | 0.049 | 4.585 | -0.418 | -0.138 | 0.270 | 0.538 | 0.602 |

Table 3: Results of the regression analyses on $V_{EIr}$ for $\mu=2$

| T[s] | a | b | c | d | e | f | h | m1 | m2 | $\tau$ | $\sigma$ | $\sigma_T$ |
|---|---|---|---|---|---|---|---|---|---|---|---|---|
| 0.10 | 6.415 | 0.283 | -0.148 | -1.958 | -0.065 | 0.114 | 13.687 | 0.051 | 0.162 | 0.292 | 0.480 | 0.561 |
| 0.20 | 5.844 | 0.636 | -0.175 | -1.330 | -0.265 | 0.053 | 10.564 | 0.017 | 0.148 | 0.201 | 0.455 | 0.497 |
| 0.30 | 5.430 | 0.664 | -0.182 | -1.263 | -0.403 | 0.061 | 7.559 | -0.074 | 0.169 | 0.196 | 0.461 | 0.501 |
| 0.40 | 5.339 | 0.650 | -0.186 | -1.387 | -0.482 | 0.085 | 6.513 | -0.147 | 0.130 | 0.210 | 0.472 | 0.517 |
| 0.50 | 5.128 | 0.621 | -0.189 | -1.483 | -0.560 | 0.106 | 5.209 | -0.176 | 0.154 | 0.215 | 0.486 | 0.531 |
| 0.60 | 4.946 | 0.615 | -0.192 | -1.537 | -0.616 | 0.119 | 4.140 | -0.187 | 0.166 | 0.222 | 0.496 | 0.544 |
| 0.70 | 4.860 | 0.603 | -0.196 | -1.615 | -0.658 | 0.132 | 3.648 | -0.190 | 0.161 | 0.231 | 0.501 | 0.552 |
| 0.80 | 4.820 | 0.598 | -0.198 | -1.681 | -0.684 | 0.143 | 3.530 | -0.215 | 0.149 | 0.240 | 0.505 | 0.559 |
| 0.90 | 4.790 | 0.593 | -0.208 | -1.739 | -0.707 | 0.151 | 3.442 | -0.214 | 0.140 | 0.250 | 0.508 | 0.566 |
| 1.00 | 4.742 | 0.596 | -0.214 | -1.785 | -0.733 | 0.159 | 3.364 | -0.236 | 0.127 | 0.262 | 0.509 | 0.572 |
| 1.10 | 4.691 | 0.642 | -0.218 | -1.757 | -0.748 | 0.154 | 3.331 | -0.207 | 0.107 | 0.266 | 0.509 | 0.574 |
| 1.20 | 4.697 | 0.662 | -0.223 | -1.774 | -0.751 | 0.156 | 3.489 | -0.229 | 0.076 | 0.265 | 0.510 | 0.575 |
| 1.30 | 4.657 | 0.693 | -0.219 | -1.757 | -0.763 | 0.153 | 3.545 | -0.239 | 0.054 | 0.261 | 0.512 | 0.575 |
| 1.40 | 4.624 | 0.712 | -0.220 | -1.753 | -0.771 | 0.152 | 3.490 | -0.207 | 0.039 | 0.264 | 0.514 | 0.578 |
| 1.50 | 4.570 | 0.739 | -0.213 | -1.739 | -0.775 | 0.150 | 3.409 | -0.201 | 0.032 | 0.262 | 0.511 | 0.574 |
| 1.60 | 4.537 | 0.755 | -0.205 | -1.740 | -0.777 | 0.149 | 3.386 | -0.210 | 0.030 | 0.259 | 0.511 | 0.573 |
| 1.70 | 4.539 | 0.745 | -0.215 | -1.757 | -0.770 | 0.152 | 3.311 | -0.190 | 0.052 | 0.264 | 0.509 | 0.573 |
| 1.80 | 4.533 | 0.741 | -0.203 | -1.790 | -0.773 | 0.156 | 3.347 | -0.189 | 0.052 | 0.260 | 0.509 | 0.571 |
| 1.90 | 4.516 | 0.749 | -0.198 | -1.796 | -0.775 | 0.156 | 3.352 | -0.198 | 0.052 | 0.257 | 0.510 | 0.571 |
| 2.00 | 4.508 | 0.752 | -0.191 | -1.810 | -0.776 | 0.157 | 3.409 | -0.193 | 0.051 | 0.257 | 0.513 | 0.573 |
| 2.20 | 4.491 | 0.763 | -0.175 | -1.832 | -0.771 | 0.159 | 3.445 | -0.209 | 0.052 | 0.254 | 0.519 | 0.578 |
| 2.40 | 4.455 | 0.774 | -0.156 | -1.832 | -0.765 | 0.158 | 3.461 | -0.228 | 0.055 | 0.251 | 0.520 | 0.578 |
| 2.60 | 4.354 | 0.894 | -0.172 | -1.662 | -0.748 | 0.134 | 3.501 | -0.267 | 0.034 | 0.251 | 0.524 | 0.581 |

| 2.80 | 4.395 | 0.917 | -0.181 | -1.673 | -0.742 | 0.134 | 3.818 | -0.282 | -0.009 | 0.250 | 0.527 | 0.583 |
| 3.00 | 4.412 | 0.934 | -0.169 | -1.676 | -0.730 | 0.133 | 3.976 | -0.257 | -0.022 | 0.234 | 0.530 | 0.580 |
| 3.50 | 4.358 | 0.989 | -0.148 | -1.611 | -0.704 | 0.122 | 4.219 | -0.234 | -0.029 | 0.224 | 0.538 | 0.583 |
| 4.00 | 4.292 | 1.016 | -0.136 | -1.552 | -0.683 | 0.114 | 4.118 | -0.271 | -0.043 | 0.217 | 0.546 | 0.587 |
| 4.50 | 4.214 | 1.080 | -0.141 | -1.474 | -0.725 | 0.102 | 3.986 | -0.263 | -0.043 | 0.212 | 0.555 | 0.594 |
| 5.00 | 4.248 | 1.057 | -0.128 | -1.533 | -0.707 | 0.109 | 3.990 | -0.235 | -0.044 | 0.205 | 0.552 | 0.588 |
| 5.50 | 4.327 | 1.031 | -0.122 | -1.590 | -0.677 | 0.115 | 4.085 | -0.242 | -0.049 | 0.209 | 0.549 | 0.587 |
| 6.00 | 4.481 | 0.922 | -0.115 | -1.789 | -0.653 | 0.141 | 4.237 | -0.240 | -0.041 | 0.210 | 0.549 | 0.588 |

Table 4: Results of the regression analyses on $V_{Elf}$ for $\mu=4$

| T[s] | a | b | c | d | e | f | h | m1 | m2 | $\tau$ | $\sigma$ | $\sigma_T$ |
|---|---|---|---|---|---|---|---|---|---|---|---|---|
| 0.10 | 6.070 | 0.394 | -0.158 | -1.704 | -0.145 | 0.095 | 11.733 | 0.029 | 0.158 | 0.229 | 0.456 | 0.510 |
| 0.20 | 5.543 | 0.638 | -0.181 | -1.318 | -0.356 | 0.064 | 8.546 | -0.048 | 0.157 | 0.189 | 0.440 | 0.479 |
| 0.30 | 5.305 | 0.635 | -0.186 | -1.402 | -0.477 | 0.087 | 6.561 | -0.122 | 0.150 | 0.198 | 0.455 | 0.497 |
| 0.40 | 5.107 | 0.630 | -0.188 | -1.487 | -0.561 | 0.106 | 5.242 | -0.170 | 0.141 | 0.210 | 0.469 | 0.514 |
| 0.50 | 4.914 | 0.626 | -0.190 | -1.555 | -0.630 | 0.121 | 4.241 | -0.191 | 0.151 | 0.222 | 0.479 | 0.528 |
| 0.60 | 4.813 | 0.632 | -0.195 | -1.619 | -0.675 | 0.133 | 3.694 | -0.215 | 0.138 | 0.233 | 0.486 | 0.539 |
| 0.70 | 4.756 | 0.638 | -0.196 | -1.673 | -0.708 | 0.141 | 3.571 | -0.238 | 0.117 | 0.243 | 0.491 | 0.548 |
| 0.80 | 4.718 | 0.639 | -0.198 | -1.733 | -0.731 | 0.150 | 3.491 | -0.266 | 0.102 | 0.251 | 0.495 | 0.555 |
| 0.90 | 4.676 | 0.656 | -0.202 | -1.748 | -0.743 | 0.152 | 3.517 | -0.258 | 0.091 | 0.249 | 0.496 | 0.554 |
| 1.00 | 4.634 | 0.685 | -0.197 | -1.748 | -0.751 | 0.151 | 3.472 | -0.278 | 0.073 | 0.250 | 0.497 | 0.556 |
| 1.10 | 4.570 | 0.718 | -0.195 | -1.735 | -0.761 | 0.149 | 3.420 | -0.217 | 0.062 | 0.249 | 0.498 | 0.557 |
| 1.20 | 4.570 | 0.734 | -0.192 | -1.750 | -0.761 | 0.150 | 3.524 | -0.227 | 0.041 | 0.249 | 0.499 | 0.557 |
| 1.30 | 4.532 | 0.754 | -0.182 | -1.749 | -0.766 | 0.149 | 3.500 | -0.233 | 0.034 | 0.248 | 0.500 | 0.558 |
| 1.40 | 4.513 | 0.763 | -0.179 | -1.760 | -0.772 | 0.150 | 3.573 | -0.201 | 0.026 | 0.252 | 0.502 | 0.562 |
| 1.50 | 4.477 | 0.780 | -0.172 | -1.752 | -0.770 | 0.149 | 3.562 | -0.201 | 0.022 | 0.246 | 0.502 | 0.559 |
| 1.60 | 4.462 | 0.788 | -0.162 | -1.760 | -0.770 | 0.149 | 3.615 | -0.203 | 0.018 | 0.244 | 0.504 | 0.560 |
| 1.70 | 4.479 | 0.772 | -0.168 | -1.781 | -0.759 | 0.152 | 3.694 | -0.182 | 0.045 | 0.246 | 0.506 | 0.562 |
| 1.80 | 4.475 | 0.779 | -0.158 | -1.796 | -0.757 | 0.153 | 3.808 | -0.185 | 0.042 | 0.242 | 0.509 | 0.564 |
| 1.90 | 4.466 | 0.781 | -0.151 | -1.800 | -0.752 | 0.153 | 3.859 | -0.184 | 0.047 | 0.239 | 0.511 | 0.564 |
| 2.00 | 4.449 | 0.786 | -0.142 | -1.800 | -0.749 | 0.152 | 3.884 | -0.185 | 0.050 | 0.236 | 0.514 | 0.565 |
| 2.20 | 4.424 | 0.803 | -0.127 | -1.796 | -0.734 | 0.151 | 3.884 | -0.208 | 0.044 | 0.228 | 0.520 | 0.567 |
| 2.40 | 4.403 | 0.806 | -0.113 | -1.800 | -0.727 | 0.150 | 3.942 | -0.217 | 0.042 | 0.224 | 0.520 | 0.566 |
| 2.60 | 4.313 | 0.914 | -0.133 | -1.642 | -0.714 | 0.128 | 3.990 | -0.271 | 0.014 | 0.223 | 0.523 | 0.569 |
| 2.80 | 4.340 | 0.925 | -0.148 | -1.654 | -0.705 | 0.130 | 4.073 | -0.278 | -0.023 | 0.224 | 0.526 | 0.571 |
| 3.00 | 4.330 | 0.929 | -0.139 | -1.654 | -0.687 | 0.129 | 3.992 | -0.249 | -0.026 | 0.215 | 0.529 | 0.571 |
| 3.50 | 4.277 | 0.950 | -0.128 | -1.607 | -0.664 | 0.122 | 3.946 | -0.251 | -0.021 | 0.217 | 0.531 | 0.574 |
| 4.00 | 4.220 | 0.964 | -0.121 | -1.560 | -0.640 | 0.116 | 3.696 | -0.283 | -0.027 | 0.214 | 0.533 | 0.574 |
| 4.50 | 4.155 | 1.015 | -0.122 | -1.508 | -0.683 | 0.108 | 3.670 | -0.265 | -0.018 | 0.200 | 0.537 | 0.573 |
| 5.00 | 4.209 | 0.964 | -0.122 | -1.592 | -0.658 | 0.119 | 3.639 | -0.258 | -0.013 | 0.198 | 0.534 | 0.569 |
| 5.50 | 4.293 | 0.910 | -0.124 | -1.676 | -0.626 | 0.130 | 3.676 | -0.268 | 0.002 | 0.211 | 0.530 | 0.571 |
| 6.00 | 4.450 | 0.777 | -0.122 | -1.908 | -0.613 | 0.161 | 3.801 | -0.262 | 0.019 | 0.214 | 0.531 | 0.572 |

**References**

[1] G. Housner, Limit design of structures to resist earthquakes. in Proceedings of the 1st World Conference on Earthquake Engineering. Berkeley, California, 1956.

[2] H. Akiyama, Earthquake Resistant Limit-State Design for Buildings (English version). Japan: University of Tokyo Press, 1985.

[3] C. M. Uang, and V. Bertero, "Evaluation of seismic energy in structures", Earthquake Engineering and Structural Dynamics, 1990, pp. 77–90.

[4] P. Fajfar, and T. Vidic, "Consistent inelastic design spectra: hysteretic and Input energy", Earthquake Engineering and Structural Dynamics, 1994, pp. 523–37.

[5] L.D. Decanini, and F. Mollaioli, "Formulation of elastic earthquake input energy spectra", Earthquake Engineering and Structural Dynamics, 1998, 27, pp. 1503–1522.

[6] C. C. Chou, and C. M. Uang, "Establishing absorbed energy spectra - An attenuation approach", Earthquake Engineering and Structural Dynamics, 2000, 29, pp. 1441-1455.

[7] M.C. Chapman, "On the use of elastic input energy for seismic hazard analysis", Earthquake Spectra, 1999, 15(4), pp. 607-635.

[8] G. Manfredi, "Evaluation of seismic energy demand", Earthquake Engineering & Structural Dynamics, 2001, 30(4), pp. 485-499.

[9] L.D. Decanini, and F. Mollaioli, "An energy-based methodology for the assessment of seismic demand", Soil Dynamics and Earthquake Engineering, 2001, 21(2), pp. 113-137.

[10] A. Benavent-Climent, L:G: Pujades F. Lopez-Almansa, "Design energy input spectra for moderate-seismicity regions", Earthquake Engineering and Structural Dynamics, 2002, 31(5), pp. 1151–1172.

[11] E. Kalkan, and S.K. Kunnath, "Relevance of absolute and relative energy content in seismic evaluation of structures", Adv. Struct. Eng., 2008, 11(1), pp. 17-34.

[12] F. Mollaioli, S. Bruno, L. Decanini, R. Saragoni, "Correlations between energy and displacement demands for performance-based seismic engineering", Pure and Applied Geophysics, 2011, 168(1-2), pp. 237-259.

[13] F. Mollaioli, A. Lucchini, Y. Cheng, and G. Monti, "Intensity measures for the seismic response prediction of base-isolated buildings", Bulletin of Earthquake Engineering, 2013, 11(5), pp. 1841-1866.

[14] Donaire-Ávila J, Mollaioli F, Lucchini A, Benavent-Climent A (2015): Intensity measures for the seismic response prediction of mid-rise buildings with hysteretic dampers. Engineering Structures, 102(2015), 278-295.

[15] Y. Cheng, A. Lucchini, F. Mollaioli, "Prediction equations for elastic input energy equivalent velocity spectra", Earthquakes and Structures, 2014, 7(4), pp. 485-510.

[16] Y. Cheng, A. Lucchini, F. Mollaioli, "Correlation of elastic input energy equivalent velocity spectral values, Earthquakes and Structures, 2015, 8(5), pp. 957-976.

[17] K.W. Campbell, Y. Bozorgnia, "NGA ground motion model for the geometric mean horizontal component of pga, pgv, pgd and 5% damped linear elastic response spectra for periods ranging from 0.01 to 10 s", Earthquake. Spectra, 2008, 24(1), 139-171.

[18] N.A. Abrahamson, and R.R. Youngs, "A stable algorithm for regression analyses using the random effects model", Bulletin of the Seismological Society of America, 1992, 82(1), 505-510.

[19] J. Pinheiro, D. Bates, S. DebRoy, and D. Sarkar, Linear and nonlinear mixed effects models. R package version 3:57, 2007.

[20] D.M. Boore, W.B. Joyner, and T.E. Fumal, "Estimation of response spectra and peak accelerations from western North American earthquakes: An interim report", U. S. Geological Survey Open-File Report 93-509, 1993.